ELSEVIER

Journal of Photochemistry and Photobiology A: Chemistry 129 (1999) 33–41

Journal of Photochemistry and Photobiology A:Chemistry

www.elsevier.nl/locate/jphotochem

Acid–base properties of bis-pyrazolopyridine derivatives in nonaqueous solutions

D. Piorun [a,*], A.B.J. Parusel [b,c], K. Rechthaler [b], K. Rotkiewicz [a,d], G. Köhler [b]

[a] *Pedagogical University of Kielce, Institute of Chemistry, Chęcińska 5, PL-25-020 Kielce, Poland*

[b] *Institut für Theoretische Chemie und Strahlenchemie der Universität Wien, Althanstrasse 14, A-1090 Vienna, Austria*

[c] *NASA Ames Research Center, MS 239-4, Moffett Field, CA 94035, USA*

[d] *Institute of Physical Chemistry, Polish Academy of Sciences, Kasprzaka 44, PL-01-224 Warsaw, Poland*

Received 14 December 1998; received in revised form 16 June 1999; accepted 19 August 1999

Abstract

Acid–base properties of four 3,5-dimethyl-1,7-diphenyl-bis-pyrazolo-[3,4-b; 4′,3′-e]-pyridine derivatives with different substituents in position 4, i.e. *N*,*N*-dimethylaminophenyl, phenyl, nitrophenyl, and methoxyphenyl (DMA-DMPP, H-DMPP, NO_2-DMPP, and CH_3O-DMPP) were investigated in nonaqueous solutions. Absorption and stationary fluorescence as well as time-resolved spectroscopy were applied as methods. The acidity of the amino group in DMA-DMPP which is preferentially protonated in the ground state, does practically not change in the first excited state. The second protonation step of DMA-DMPP and the protonation of the other compounds occurs at the heterocyclic subunit, in the ground state most probably on the pyridine nitrogen. The basicity of this nitrogen atom increases remarkably in the first excited state. Experimental results were compared with those of semiempirical calculations. The amino group as the preferential site of protonation before the pyridine nitrogen in the ground state was confirmed. According to quantum mechanical computations, one pyrazolo nitrogen is preferentially protonated in the first excited state. The protonation is accompanied by a geometrical relaxation leading to a planarized conformer with a lower total energy.

Keywords: Acid–base equilibria; bis-Pyrazolopyridines; Hydrogen-bonding; Charge transfer; Fluorescence; Semiempirical calculations

1. Introduction

Donor–acceptor substituted aromatic organic compounds have generally highly dipolar charge-separated excited states and are, therefore, suitable candidates for high second order nonlinear optical properties [1]. For a high second order polarizability a large transition dipole moment, and a large difference between ground and excited state dipole moment are unalterable prerequisites. Large π-conjugated systems substituted with both a strong electron donor and acceptor exhibit enhanced nonlinear optical (NLO) properties [2]. The formation of a highly polar charge transfer state of DMA-DMPP makes this class of systems a promising candidate for highly efficient NLO chromophores [3–5].

Derivatives of 3,5-dimethyl-1,7-diphenyl-bis-pyrazolo-[3,4-b;4′,3′-e]-pyridine with different substituents in position 4 (see Section 1.1) are compounds showing intense fluorescence in the blue-green region and are considered for application as fluorescence standards and luminophors in organic light-emitting diodes.

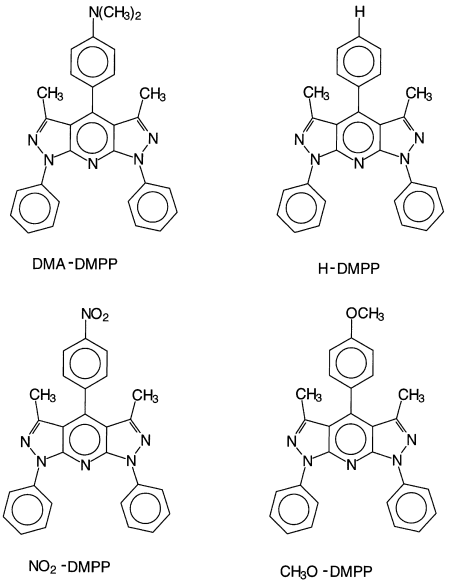

* Corresponding author.

1010-6030/99/$ – see front matter
PII: S1010-6030(99)00182-3

The derivatives with phenyl and 4-methoxyphenyl substituent (H-DMPP and CH_3O-DMPP, respectively) are characterized by a very intense, solvent-independent fluorescence. The nitro derivative (NO_2-DMPP) shows an unexpected photophysical behaviour. A peculiar stabilization of the two lowest excited singlets, depending on solvent polarity, leads to dual fluorescence [6]. DMA-DMPP is a molecule composed of a dimethylanilino donor and a large π-electron acceptor subunit linked by a single bond. The subunits are noncoplanar, the angle between their planes is ca. 77° in the ground state [3]. DMA-DMPP fluoresces with a large quantum yield in nonpolar solvents. The quantum yield decreases in polar solvents, and the emitting state changes its character from a weakly polar to a CT one, confirmed by experimental results [4,5,7–9]. In protic solvents dual fluorescence is observed, a phenomenon not often occurring in the case of noncoplanar large donor–acceptor systems. Between both emission bands no precursor–successor relationship exists, as their excitation spectra differ. The long-wavelength band was ascribed to the CT emission [7–9]. The results of the picosecond time-resolved measurements of the excited states dynamics of DMA-DMPP in methanol [7,8] show that the main fraction of the excited molecules undergoes rapid relaxation to the CT state in <10 ps after excitation at room temperature. The nature of the species emitting the short-wavelength band is not yet explained definitely. We can ascribe it tentatively to hydrogen-bonded molecules. For a better understanding of the interaction of the DMA-DMPP molecule with a proton we have undertaken investigations of the acid–base properties of this molecule and the other 4-substituted derivatives. These compounds are additionally interesting with respect to investigations of their protolytic reactions due to the existence of different protonation centers.

The measurements were performed in nonaqueous solutions, i.e. in acetonitrile and ethanol as solvents because of the sparing solubility of the compounds in water.

2. Materials and methods

2.1. Experimental section

The four investigated compounds DMA-DMPP, H-DMPP, NO_2-DMPP, and CH_3O-DMPP were synthetized in the Department of Organic Chemistry of the Institute of Chemistry of the Pedagogical University in Kielce, Poland [3,9].

The solvents and $HClO_4$ (60% w/w) used were of the highest available quality and checked for impurities by means of absorption and fluorescence spectroscopy.

Absorption and fluorescence emission spectra as well as fluorescence decay times were measured as described previously [9]. The fluorescence excitation spectra were measured with a Kontron SFM 25 spectrofluorimeter.

2.2. Semiempirical calculations

Semiempirical calculations were performed with VAMP6.1 [10] on a SGI INDY (MIPS R4400) at the University of Vienna. Standard AM1 [11] parameters were used throughout the work. All AM1 geometries were optimized in the electronic ground state, and the conformation with various torsion angles α between the donor and the acceptor unit was optimized as well. These geometries have been used for configuration interaction with single and double excitations (CISD) with an active space of 10 orbitals, corresponding to 876 configurations used in the configuration interaction (CI). For solute–solvent interactions the self consistent reaction field (SCRF) [12] was applied.

3. Results

3.1. Absorption spectra and acid–base properties of the ground state

The absorption spectrum of DMA-DMPP in acetonitrile solution changes remarkably upon the addition of even a small amount of perchloric acid. The absorption coefficient (ε) of the two longest-wavelength absorption bands (peaking at 26 500 and 30 500 cm^{-1}) decreases (Fig. 1(a)). Well-defined isosbestic points are observed at 35 600, 38 600, and 43 000 cm^{-1}. At a molar concentrations ratio of DMA-DMPP/$HClO_4$ = 1 : 1 the long-wavelength part of the spectrum looks like that of H-DMPP without $HClO_4$ (compare Fig. 1(a) and Fig. 2(a)). The increase of the acid concentration above 2.5×10^{-5} M causes further changes of absorption (see Fig. 1(b)) A new band appears at the long-wavelength side of the spectrum, peaking below 26 000 cm^{-1}. New isosbestic points are observed at 26 700, 29 300, 33 000, 36 900, 40 400, and 45 300 cm^{-1}.

The absorption changes of the acidified acetonitrile solutions of the H-DMPP and NO_2-DMPP (Fig. 2(a,b)) closely resemble that of DMA-DMPP (Fig. 1(b)) in the region of $HClO_4$ concentrations larger than 2.5×10^{-5} M.

The changes of the absorption spectrum of DMA-DMPP in ethanol at the first step of acidification (Fig. 3) is similar to that in acetonitrile (Fig. 1(a)). However, the same change of absorption needs larger concentrations of acid than in acetonitrile. At concentrations larger than 0.1 M no further changes occur. In the case of other compounds practically no changes in absorption are observed.

3.2. Fluorescence spectra: protolytic properties of the first excited singlet state

The changes of the fluorescence spectra of DMA-DMPP in acetonitrile solutions upon addition of $HClO_4$ are depicted in Fig. 4(a,b). With increasing acid concentration the short-wavelength band increases. It reaches its largest

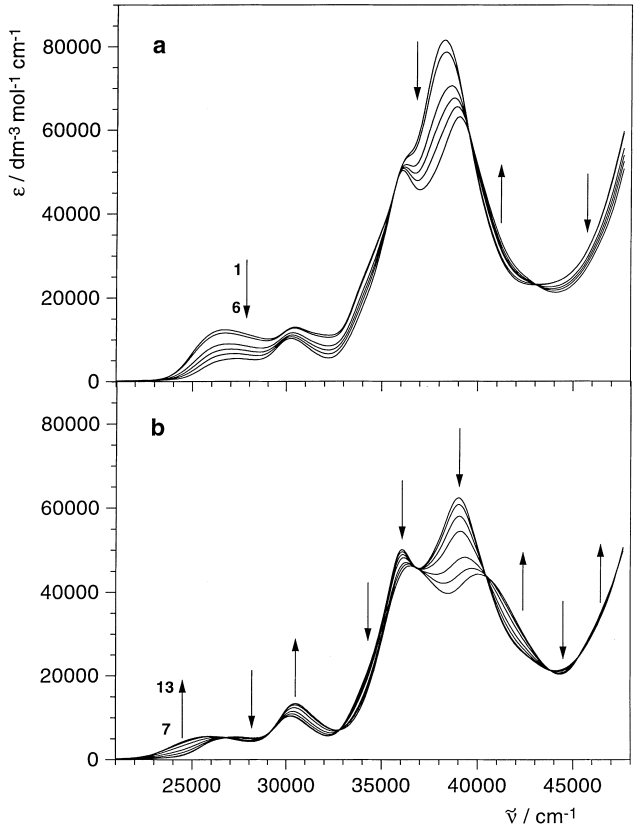

Fig. 1. Absorption spectra of acidified DMA-DMPP solutions in acetonitrile ($c = 1.94 \times 10^{-5}$ M): (a) acid ($HClO_4$) concentrations from 0 M (1), 3.88×10^{-6} M (2), 1.16×10^{-5} M (3), 1.55×10^{-5} M (4), 1.75×10^{-5} M (5), 1.94×10^{-5} M (6); (b) 3.88×10^{-5} M (7), 9.70×10^{-5} M (8), 1.94×10^{-4} M (9), 3.88×10^{-4} M (10), 9.70×10^{-4} M (11), 1.94×10^{-3} M (12), 5.82×10^{-3} M (13). The arrows denote the direction of the absorbance changing with increasing acid concentration from 1 to 6 (Fig. 1(a)) and from 7 to 13 (Fig. 1(b)).

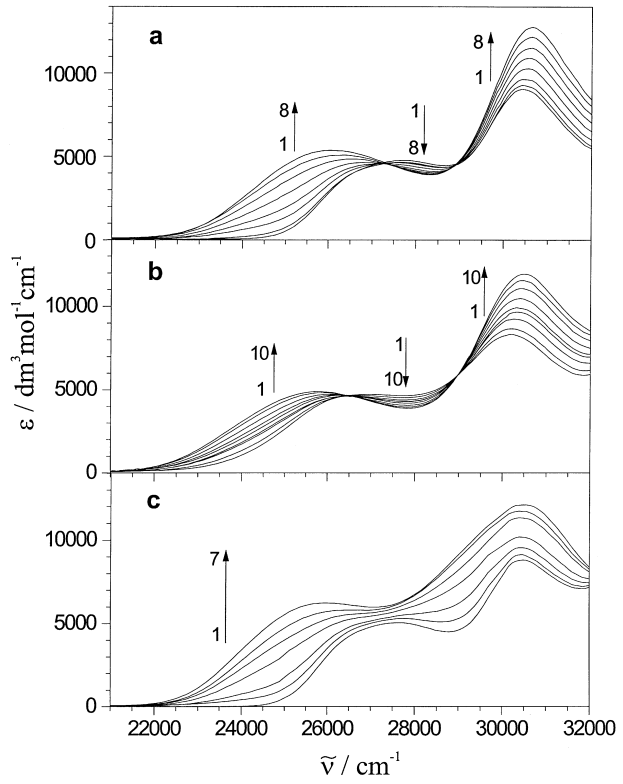

Fig. 2. Absorption spectra of acidified acetonitrile solutions of: (a) H-DMPP ($c = 5 \times 10^{-5}$ M), $HClO_4$ concentrations: 0 M (1), 5.0×10^{-5} M (2), 1.0×10^{-4} M (3), 1.5×10^{-4} M (4), 8.5×10^{-4} M (5), 3.6×10^{-3} M (6), 1.3×10^{-2} M (7), 6.1×10^{-2} M (8). (b) NO_2-DMPP ($c = 6.4 \times 10^{-5}$ M), $HClO_4$ concentrations: 0 M (1), 1.3×10^{-4} M (2), 1.9×10^{-4} M (3), 2.5×10^{-4} M (4), 4.5×10^{-4} M (5), 1.2×10^{-3} M (6), 1.8×10^{-3} M (7), 2.8×10^{-3} M (8), 5.9×10^{-3} M (9), 2×10^{-2} M (10). (c) CH_3O-DMPP ($c = 4.8 \times 10^{-5}$ M), $HClO_4$ concentrations: 0 M (1), 1.2×10^{-4} M (2), 1.8×10^{-4} M (3), 2.4×10^{-4} M (4), 5.9×10^{-4} M (5), 1.5×10^{-3} M (6), 3.2×10^{-2} M (7).

quantum yields at ca. 2.5×10^{-5} M $HClO_4$, at which the ratio of the molar concentrations DMA-DMPP : $HClO_4$ is ca. 1 : 1. The excitation spectra of the short- and long-wavelength fluorescence bands in acidified solutions are distinctly different (Fig. 5).

At the region of the second protonation, i.e. at acid concentrations from 2.5×10^{-5} to 7.5×10^{-3} M, the single fluorescence band of monoprotonated DMA-DMPP decreases (Fig. 4(b)). A slight trace of some long-wavelength band appears below 17 000 cm^{-1}.

In the case of acidified solutions of H-DMPP, CH_3O-DMPP, and NO_2-DMPP the fluorescence quenching is mainly observed (Fig. 6(a–c)). A new weak long-wavelength band also appears. It is most distinctly seen for the nitro compound (Fig. 6(b)).

The fluorescence decay time τ_f in acetonitrile solution at 298 K is 19.6 ns. It depends remarkably on temperature. Upon acidification with $HClO_4$, at large concentrations of acid (Table 1) when the amino group in the ground state is completely protonated (see the absorption spectra in Fig. 1) and the bication occurs, τ_f increases up to (27 ± 2) ns.

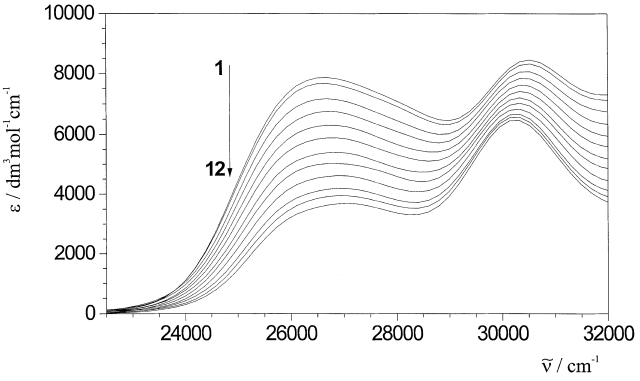

Fig. 3. Absorption spectra of acidified ethanol solutions of DMA-DMPP ($c = 2.65 \times 10^{-5}$ M), $HClO_4$ concentrations: 0 M (1), 5.3×10^{-4} M (2), 1.6×10^{-3} M (3), 2.65×10^{-3} M (4), 4.0×10^{-3} M (5), 5.3×10^{-3} M (6), 7.95×10^{-3} M (7), 1.06×10^{-2} M (8), 1.6×10^{-2} M (9), 2.65×10^{-2} M (10), 4.0×10^{-2} M (11), 8.0×10^{-2} M (12).

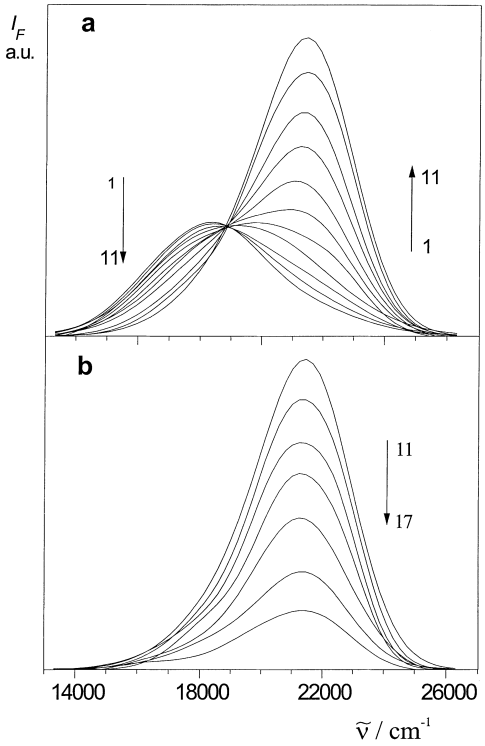

Fig. 4. Corrected fluorescence spectra in acidified acetonitrile solutions of DMA-DMPP ($c = 2.5 \times 10^{-5}$ M): (a) acid concentration from 0 (1) to 2.5×10^{-5} M (11) in steps of 0.25×10^{-5} M; (b) 2.5×10^{-5} M (11), 5.0×10^{-4} M (12), 1.0×10^{-3} M (13), 1.5×10^{-3} M (14), 2.5×10^{-3} M (15), 5.0×10^{-3} M (16), 7.5×10^{-3} M (17); $\lambda_{exc} = 373$ nm.

Monoexponential fitting describes the decay kinetics in all cases.

Solutions of DMA-DMPP in ethanol show a remarkable increase of the short-wavelength band of fluorescence upon addition of acid up to 1.6×10^{-2} M (Fig. 7(a)). Further addition of acid leads to mere quenching of fluorescence (Fig. 7(b)). The fluorescence of the three other derivatives is mainly quenched on acidification in solutions in ethanol, similarly like in the case of solutions in acetonitrile.

Table 1
Fluorescence lifetimes of DMA-DMPP ($c = 2.5 \times 10^{-5}$ M) in acidified acetonitrile solutions, $\lambda_{exc} = 370$ nm

[H$^+$]/[DMA-DMPP]	λ_{em} (nm)	τ_f (ns)
0	540	19.6
0.6	478	24.6
	515	20.9
	550	19.3
22.0	469	25.9
	515	27.2
	550	28.1

Table 2
Fluorescence lifetimes of DMA-DMPP in neat alcohols

	Short-wavelength emission[a]		Long-wavelength emission[b]	
	τ_f (ns)	a[c]	τ_f (ns)	a
Methanol	0.4	0.004	1.3	0.026
	25	0.001	26	0.0007
Ethanol	0.2	0.032	0.3	−0.023
	6.4	0.0026	3.5	0.023
Propanol-1	0.1	0.138	0.6	−0.0016
	6.7	0.0047	5	0.0049
Butanol-1	<0.1	1.118	1	−0.0023
	6.9	0.0176	6.4	0.0139

[a] The short-wavelength emission between 440 and 445 nm.
[b] The long-wavelength emission between 540 and 590 nm.
[c] Denotes the pre-exponential factor.

The decay kinetics even in neat alcohol is rather complex. It is biexponential monitored both at short and at long wavelengths. With increasing chain length of the alcohol the following effects are observed (see Table 2):

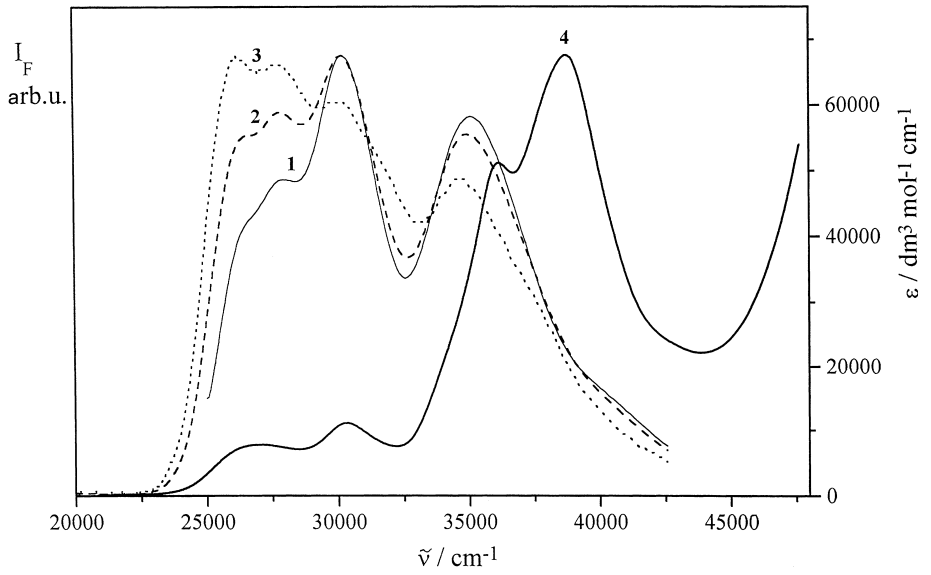

Fig. 5. Uncorrected excitation spectra of DMA-DMPP ($c = 1.94 \times 10^{-5}$ M) in acetonitrile solution with 1.55×10^{-5} M $HClO_4$: spectra at $\lambda_{em} = 420$ nm (1), 520 nm (2), 625 nm (3); for comparison with the absorption spectrum of this solution (4).

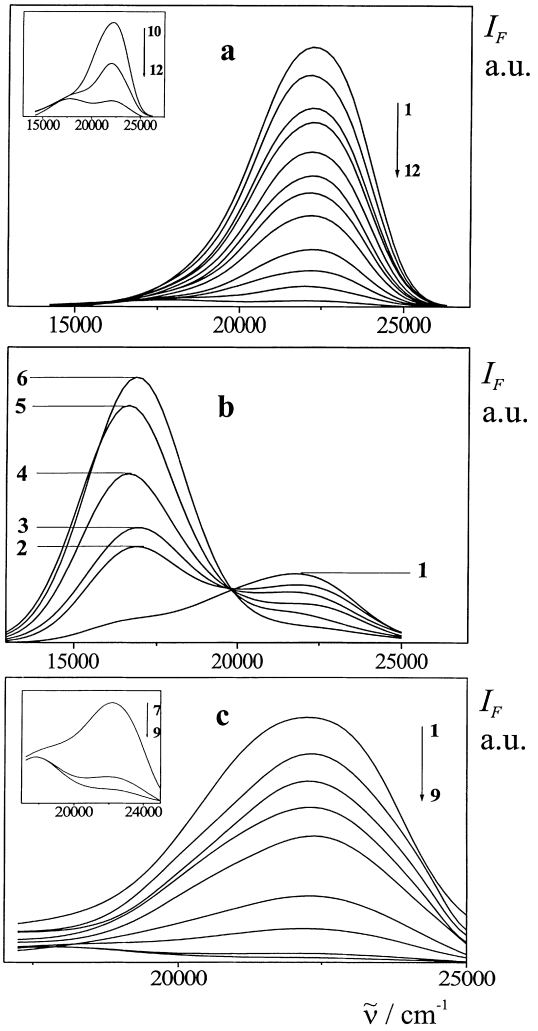

Fig. 6. Corrected fluorescence spectra in acidified acetonitrile solutions of: (a) H-DMPP ($c = 5.5 \times 10^{-5}$ M), $HClO_4$ concentrations: 0 M (1), 5.5×10^{-5} M (2), 1.1×10^{-4} M (3), 1.6×10^{-4} M (4), 2.8×10^{-4} M (5), 3.8×10^{-4} M (6), 5.5×10^{-4} M (7), 8.2×10^{-4} M (8), 1.6×10^{-3} M (9), 2.8×10^{-3} M (10), 5.5×10^{-3} M (11), 1.6×10^{-2} M (12), inserted the enlarged spectra 10 to 12 at $\lambda_{exc} = 380$ nm; (b) NO_2-DMPP ($c = 3.7 \times 10^{-5}$ M), $HClO_4$ concentrations: 0 M (1), 7.4×10^{-4} M (2), 1.1×10^{-3} M (3), 1.8×10^{-3} M (4), 3.7×10^{-3} M (5), 1.1×10^{-2} M (6) at $\lambda_{exc} = 368$ nm; (c) CH_3O-DMPP ($c = 3.8 \times 10^{-5}$ M), $HClO_4$ concentrations: 0 M (1), 1.9×10^{-4} M (2), 3.8×10^{-4} M (3), 5.7×10^{-4} M (4), 7.6×10^{-4} M (5), 1.9×10^{-3} M (6), 3.8×10^{-3} M (7), 1.1×10^{-2} M (8), 1.9×10^{-2} M (9), inserted the enlarged spectra 7 to 9 at $\lambda_{exc} = 370$ nm.

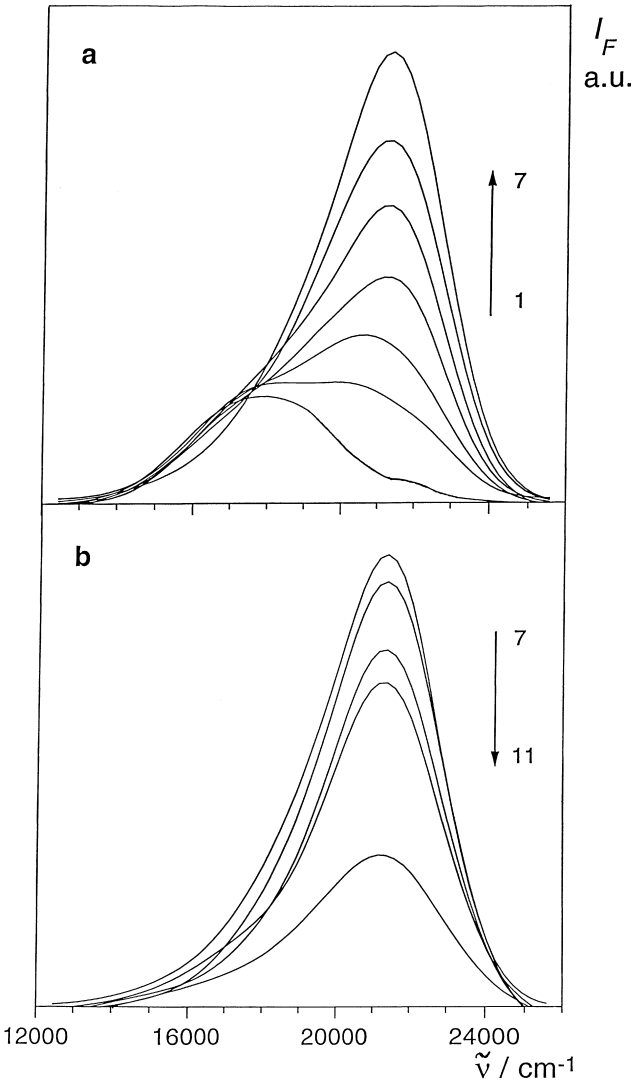

Fig. 7. Corrected fluorescence spectra ($\lambda_{exc} = 375$ nm) in acidified ethanol solutions of DMA-DMPP ($c = 2.65 \times 10^{-5}$ M): (a) acid concentrations: 0 M (1), 1.6×10^{-3} M (2), 2.65×10^{-3} M (3), 4.0×10^{-3} M (4), 5.3×10^{-3} M (5), 8.0×10^{-3} M (6), 1.6×10^{-2} M (7); (b) 1.6×10^{-2} M (7), 2.65×10^{-2} M (8), 4.0×10^{-2} M (9), 5.3×10^{-2} M (10), 0.13 M (11).

(a) in the short-wavelength band (440–445 nm): a decrease of the short-lived component from 0.4 ns down to below 0.1 ns and an initially dramatic decrease of the long-lived component from 25 ns in methanol to values of 6–7 ns in the further alcohols.

(b) in the long-wavelength band (540–590 nm): an increase of the short-lived component showing negative amplitude with methanol as exception. Neither its value nor its amplitude correlate with the short-lived component of short-wavelength emission. Also, most probably the equality of the corresponding amplitudes in ethanol is a mere accident. The long-lived component increases, also with methanol as an exception. Most probably this 26 ns component stems from the same species observed in the short-wavelength region and corresponds to the decay time of the monocation in acetonitrile (see Table 1).

τ_f in acidified ethanol solutions can be characterized by experimental facts (see Table 3) as follows:

1. usually biexponential decay: the short-lived component corresponds to nonprotonated species. It is equal to that in neat ethanol at small acid concentrations and shows proton quenching at high concentrations of acid. The long-lived component can be ascribed to protonated species. Maybe protonation occurs already in the case of neat methanol to a small extent (see Table 2).

Table 3
Fluorescence lifetimes of DMA-DMPP ($c = 2.5 \times 10^{-5}$ M) in acidified ethanol solutions, $\lambda_{exc} = 370$ nm

$[H^+]/[DMA\text{-}DMPP]$	λ_{em} (nm)	τ_f (ns)	Percentage[a]
20	469	3.5	5
		24	95
	522	3.5	28
		20	72
250	476	18	100
	532	2.5	13
		19	87
	555	2.6	23
		19	77
600	469	16	100
	522	1.6	1
		15	99
	562	1.9	10
		11	90

[a] The percentage of total yield was calculated according to $a_i\tau_{f,i}/\Sigma a_i\tau_{f,i}$, where a_i denotes the pre-exponential factor of the corresponding lifetime $\tau_{f,i}$.

2. The charge transfer fluorescence is proton-quenched. τ_f decreases from 3.5 ns in neat ethanol to 1.6 ns at large excess of acid ($\approx 10^{-2}$ M).
3. Accordingly (observed at short wavelengths with large excess of acid) the short-lived component (CT fluorescence) cannot be resolved clearly so that the decay remains essentially monoexponential.
4. The long-lived component, ca. 20 ns at $HClO_4$ concentration ca. 5×10^{-4} M, is shortened to ca. 11–15 ns at $\approx 10^{-3}$ M $HClO_4$ concentration.

The excitation spectra of the fluorescence of protonated and nonprotonated species are different, similarly to the case of solutions in acetonitrile. Moreover, in neat ethanol the fluorescence excitation spectrum of the short-wavelength fluorescence differs from that of the long-wavelength one. The former resembles that of the protonated form.

3.3. Semiempirical calculations

Investigation of the ground state coordinate of DMA-DMPP along the rotational angle α about the single bond connecting the phenyl group in 4-position and the heteroaromatic part yields in a minimum conformation for the ground state with almost decoupled donor and acceptor subunits ($\alpha \approx 77^\circ$). The most stable conformation is unchanged for protonation at the amino group and changed to an angle of $\alpha = 50^\circ$ when either the pyrazolo or pyridine nitrogen group are protonated. A significant increase in total energy is determined for rotational angles α smaller than 50°, i.e. for more planarized molecules. The net atomic charges show a large negative value located at the amino nitrogen. In the pyridine as well as in the pyrazolo rings the charge on the nitrogens is significantly smaller than that of the amino nitrogen. The pyrazolo nitrogens show a relatively small negative charge which almost disappears in polar solvents, thus increasing the effect described before. Also, for the first excited state a stabilization in energy is computed for flattened systems with an energy minimum for $\alpha = 40^\circ$ at all three protonation sites along this rotation: It equals 25 kJmol^{-1} for the pyrazolo, 21 kJmol^{-1} for the amino, and 17 kJmol^{-1} for the pyridine site protonation.

Two general statements can be derived. First, the protonation at the amino position leads to the most stable system and protonation at the pyrazolo nitrogen is the next step in the ground state. Second, the protonation causes a stabilization of the more conjugated system, i.e. flattened geometries with a minimum conformation at $\alpha = 40^\circ$.

4. Discussion

4.1. Absorption spectra

The absorption spectra of H-DMPP, CH_3O-DMPP, and NO_2-DMPP are similar to one another. The second band is more intense than the first one. The spectrum of DMA-DMPP in polar solvents differs from the others and shows similar absorption coefficients for both bands (Fig. 1). The difference between DMA-DMPP and the three other derivatives is due to the auxochromic effect of the *N*,*N*-dimethylamino group, thus enlargening the π-electronic system.

The decrease of the first absorption band and its blue-shift on protonation are unambiguously caused by the protonation of the amino group. Thus, the lone pair of the amino nitrogen atom is no longer available for the π-system. The isosbestic points indicate an equilibrium between the monocation and the nonprotonated form in the ground state. The monocation of DMA-DMPP, i.e. protonated on amino nitrogen, undergoes further protonation upon acidifying of the solution in acetonitrile. A new red-shifted band appears (Fig. 4(b)). New isosbestic points indicate the protonation of a heterocyclic nitrogen atom and an equilibrium between mono- and biprotonated form.

The sequence of the protonation steps is in accordance with the results of the quantum mechanical calculations, i.e. the protonation of the amino nitrogen is followed by that on pyridine nitrogen. The second protonation step may be retarded, as the pyridine nitrogen is sterically hindered by both phenyl groups and can be reached only with difficulties by a solvated proton.

H-DMPP and NO_2-DMPP with pyrazolo protonation centers show absorption changes similar to those of DMA-DMPP at the second protonation step (compare Fig. 2(a,b) with Fig. 1(b)). The increase of the absorbance on the long-wavelength shoulder of the first absorption band, accompanied by its red-shift, is observed in the case of CH_3O-DMPP, too, but without isosbestic points. This nonexistence can possibly be ascribed to an additional interaction between the methoxy oxygen atom and the proton.

4.2. Fluorescence spectra

The short-wavelength fluorescence band peaking at 21 500 cm^{-1} which occurs in acidified DMA-DMPP solutions in acetonitrile can be ascribed to the form protonated at the *N*,*N*-dimethylamino group. The fluorescence of nonprotonated DMA-DMPP peaks at 18 200 cm^{-1}.

A practically unchanged acidity of the amino group in excited state is found. At the concentration of $HClO_4$ at which the amino group is totally protonated in the ground state only the blue-shifted intense fluorescence from protonated molecule is emitted. In solutions in which the fluorescence of protonated and nonprotonated forms is observed, the excitation spectra of both fluorescence bands differ remarkedly (Fig. 5). It provides a strong argument for the lack of deprotonation of DMA-DMPP, protonated at the amino nitrogen in excited state. Moreover, it means that the *N*,*N*-dimethylamino subunit is isolated from the excited system. According to theoretical calculations the S_1 is localized on the bis-pyrazolopyridine moiety due to the strong decoupling of both subunits. The change of the absorption and fluorescence of the same magnitude occurs at higher concentration of $HClO_4$ in ethanol than in acetonitrile due to the basicity difference of those solvents.

A well-defined isoemissive point is observed at 18 800 cm^{-1}, but it should reflect the protolytic equilibrium in ground state due to the difference of excitation spectra of both fluorescence bands. However, the fluorescence spectra were measured by excitation at the maximum of the first absorption band, i.e. at 26 500 cm^{-1}. The absorption at this wavelength decreases more than twice at an acid concentration of 2.5×10^{-5} M. Thus, the isoemissive point can exist only in that case, in which the decreasing concentration of excited molecules (due to the decreasing absorption) will be compensated by some other features, i.e. by a concomitant increase of quantum yield.

Measurable absorption changes corresponding to the second step of protonation of DMA-DMPP and to the first step of the other three compounds was observed only in acetonitrile in the presence of $HClO_4$ concentration under study, i.e. up to 0.1 M. These protonations lead to a decrease of the fluorescence quantum yield (Fig. 4(b)). At the present stage, we cannot identify the quenching mechanism. Further investigations, if a proton quenching of the nonprotonated heterocycle or the formation of a nonfluorescent protonated form is responsible, are under study. Thus, in Scheme 1 we mark the protonation in excited state by dashed lines.

A new weak band arises at 19 800 cm^{-1}. In the case of DMA-DMPP only a trace of this band is seen at the highest used $HClO_4$ concentrations (Fig. 4(b)). This band could be tentatively ascribed to the fluorescence of a form protonated on a heterocyclic nitrogen atom. In the case of NO_2-DMPP an alternative explanation of this weak fluorescence can be related to the dual fluorescence observed in medium polar solvents and ascribed to the emission from another excited state stabilized in these solvents [6]. A nonexistence of protolytic reaction between free molecule and that on amino group protonated form of DMA-DMPP in the S_1 state is observed in ethanol as solvent. The fluorescence of both forms decays independently (Table 3) as the sum of two exponents. The fluorescence from CT state of nonprotonated molecules shows a known quenching effect by proton, its decay time decreases with increasing $HClO_4$ concentration. The protonated form is quenched, too. This deactivation channel is absent in acetonitrile. Although the protonation of heterocyclic nitrogen atoms was not observed in the ground state in ethanol, a fluorescence quenching takes place (Fig. 7).

4.3. Thermodynamic stability of the protonated species

The changes of ΔpK_a (= pK_a^*–pK_a) in the excited singlet state for the forms protonated on the heterocyclic nitrogen atoms were estimated by means of Förster's cycle for the solutions in acetonitrile. The estimations of the upper limit of $\Delta pK_a \approx 7$ units were based on the assumption that the weak long-wavelength fluorescence bands, observed in strongly acidified solutions, correspond to the emission of the cation, and on the shift of those fluorescence maxima. On the other hand, the estimations of the lower limit were based on the shift of the maxima of the longest-wavelength absorption, assuming that it is the first absorption band and the fluorescence of the protonated forms are absent. In this case ΔpK_a is remarkedly smaller and decreases in the following sequence (in parentheses ΔpK_a): NO_2-DMPPH$^+$ (2,2) < DMA-DMPPH_2^{2+} (2,7) < H-DMPPH$^+$ (3,5) < CH_3O-DMPPH$^+$ (3,6).

This correlates with the electronic properties of the 4′-substituent. The stronger the electron acceptor, the smaller the change of acidity. The uncertainities of the ΔpK_a are large ($\approx$0.5 units), so the differences are almost within error limits.

The stability of the monocation of DMA-DMPP in its first excited state may be useful for the explanation of the source of the dual fluorescence of DMA-DMPP in neat alcohols. The dynamics of excited DMA-DMPP molecules in alcohols is rather complex, reflected in fluorescence decay (Table 2). The decay components in the short-wavelength band shows the existence of at least two hydrogen-bonded species. There is no correlation to the decay components in the long-wavelength band. The lack of the precursor–successor relation is corroborated by (i) different fluorescence excitation spectra, (ii) the results of the picosecond time-resolved measurements of DMA-DMPP in methanol [7,8]. The main fraction of excited molecules undergoes rapid relaxation to the CT state. The charge separation is faster than the dynamics of the Stokes shift. By analogy to the preferential protonation of the amino group of DMA-DMPP in the ground state, the preferential formation of hydrogen-bonded complexes is also expected there. On one hand, these complexes do not dissociate in the excited state due to the unchanged acidity of the amino

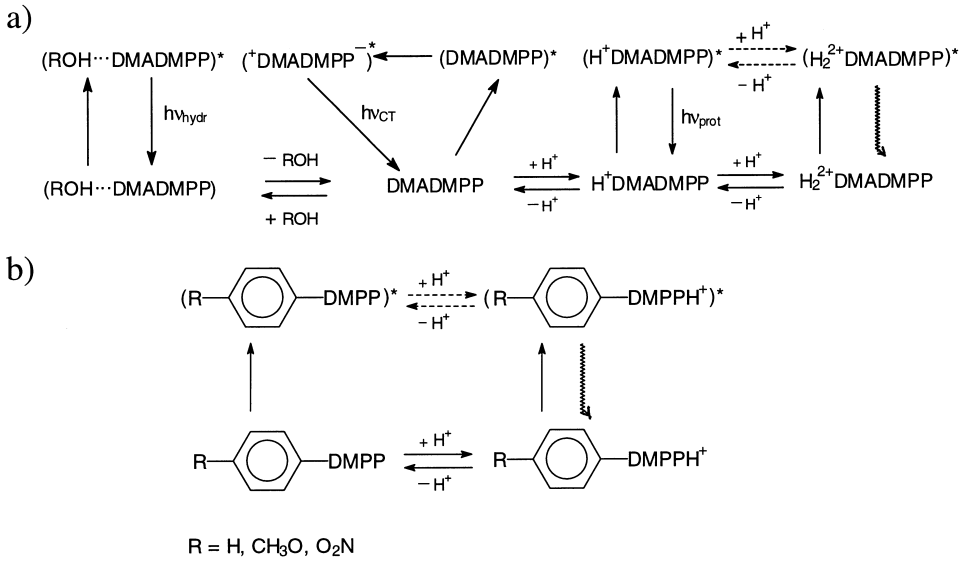

Scheme 1. (a) Hydrogen-bonding and protonation equilibria in ground and excited state for DMA-DMPP. $h\nu_{hydr}$ denotes the fluorescence from the hydrogen-bonded molecules, $h\nu_{CT}$ from the charge-separated state, and $h\nu_{prot}$ from the monoprotonated form; (b) Protonation equilibria in ground and excited state for H-DMPP, CH_3O-DMPP, and NO_2-DMPP.

group. The stability of the cation in the S_1 state suggest the stability of the hydrogen-bonded form and its unability to relax to the CT state during the lifetime of the excited state. In the case of methanol solution there is no indication for the relaxation of these species to the CT state (lack of any rise time component at long wavelengths, Table 2). Moreover, the slow component of the decay closely resembles the decay time of DMA-DMPP cation both in acetonitrile and ethanol (compare Tables 1–3). On the other hand, the hydrogen-bonded complexes to the pyridine nitrogen should appear in the excited state due to the increased basicity of this atom. This process is relatively slow (several tens of picoseconds) but such complexation leads to an increase of the electron affinity of the acceptor subunit.

Anyway, the results of DMA-DMPP protonation study as well as the decay kinetics in neat alcohols suggest the existence of at least two different species in the electronic ground state, responsible for the dual fluorescence in protic solvents. On the basis of the above given results and considerations, we propose the following scheme of hydrogen-bonding and protonation equilibria in ground and excited states for those four compounds (Scheme 1).

5. Conclusions

1. DMA-DMPP is a molecule with potentially three different protonation centers. The protonation takes place in two steps: at first on the amino group, secondly on one of the heterocyclic nitrogen atoms, most probably on the pyridine one, as it is shown by theoretical results.
2. The protonation occurs much easier in acetonitrile solutions than in ethanol ones. The total protonation of the amino group takes place already at solute/$HClO_4$ molar concentrations ratio 1 : 1 and ≈1 : 2000 in acetonitrile and ethanol, respectively.
3. The H-, NO_2- and CH_3O-derivatives undergo protonation at one of the heterocyclic nitrogen atoms at similar $HClO_4$ concentrations in acetonitrile as for DMA-DMPP reaction in the second step. In ethanol no indication of such protonation is observed up to a $HClO_4$ concentration of 0.1 M.
4. The *N,N*-dimethylamino group in DMA-DMPP practically does not change its acidity upon excitation to the S_1 state. The fluorescence spectra reflect the ground state protolytic equilibrium at the first step.
5. By an excess of acid concentration in acetonitrile solution the pyridine nitrogen is protonated most probably. Its basicity increases remarkably in the S_1 state.
6. The stability of DMA-DMPP cation in the first excited state corroborates the ascribing of the dual fluorescence of DMA-DMPP in protic solvents to the emission from the free and hydrogen-bonded form.

Acknowledgements

The authors are indebted to Prof. Danuta Rasała and Ms. Sci. Agnieszka Puchała (Kielce, Poland) for providing the samples of the investigated compounds as well as to Prof. Zbigniew R. Grabowski (Warsaw, Poland) for valuable remarks. The work was done in the framework of Project No. 01-003 and 06/R98/R99 included to Austrian–Polish Convention of Scientific and Technological Cooperation. The *Fonds zur Förderung der Wissenschaftlichen Forschung in Österreich* (Project No. P11880-CHE) and the Committee

for Sci. Research in Poland (grant 8T11b00510) are gratefully acknowledged for financial support. *Volkswagen Foundation*, Germany, is acknowledged for providing the Kontron SFM 25 spectrofluorimeter to W. Iwanek (Institute of Pedagogical University, Kielce, Poland). A. Parusel thanks the German Academic Exchange Service (DAAD) for a postdoctoral fellowship.

References

[1] C. Bosshard, K. Sutter, P. Prêtre, J. Hulliger, M. Flörsheimer, P. Kaatz, P. Günter, Organic Nonlinear Optical Materials, Gordon and Breach Publishers, Basel, 1995.
[2] D. Kanis, M. Ratner, T. Marks, Chem. Rev. 94 (1994) 195.
[3] A.B.J. Parusel, R. Schamschule, D. Piorun, K. Rechthaler, A Puchała, D. Rasała, K. Rotkiewicz, G. Köhler, J. Mol. Struct. (Theochem.) 419 (1997) 63.
[4] A.B.J. Parusel, R. Schamschule, G. Köhler, Ber. Bunsenges, Phys. Chem. 101 (1997) 1836.
[5] A.B.J. Parusel, R. Schamschule, G. Köhler, J. Comput. Chem. 19 (1998) 1584.
[6] K. Rechthaler, R. Schamschule, A.B.J. Parusel, K. Rotkiewicz, D. Piorun, G. Köhler, Acta Phys. Polon. A 95 (1999) 321.
[7] H. Miyasaka, A. Itaya, K. Rotkiewicz, Picosecond dynamics of excited states of DMA-DMPP, highly emissive and TICT forming compound, 17th IUPAC Symposium on Photochemistry, Sitges (Barcelona, Spain), July 19–24, 1998, Book of Abstracts, p. 112.
[8] H. Miyasaka, A. Itaya, K. Rotkiewicz, K. Rechthaler, Chem. Phys. Lett., 307 (1999) 121.
[9] K. Rotkiewicz, K. Rechthaler, A. Puchała, D. Rasała, S. Styrcz, G. Köhler, Photochem. Photobiol. A: Chem. 98 (1996) 15.
[10] G. Rauhut, A. Alex, J. Chandrasekhar, T. Steinke, W. Sauer, B. Beck, M. Hutter, P. Gedeck, T. Clark, VAMP6.1, Oxford Molecular Ltd., Oxford, 1997.
[11] M.J.S. Dewar, E.G. Zoebisch, E.F. Healy, J.J.P. Stewart, J. Am. Chem. Soc. 107 (1985) 3902.
[12] G. Rauhut, T. Clark, T. Steinke, J. Am. Chem. Soc. 115 (1993) 9174.